



**HAL**  
open science

**The inducible  $\beta 5i$  proteasome subunit contributes to proinsulin degradation in GRP94 deficient  $\beta$  cells and is overexpressed in type 2 diabetes pancreatic islets**

Muhammad Saad Khilji, Sophie Emilie Bresson, Danielle Verstappen, Celina Pihl, Phillip Alexander Keller Andersen, Jette Bach Agergaard, Tina Dahlby, Tenna Holgersen Bryde, Kristian Klindt, Christian Kronborg Nielsen, et al.

► **To cite this version:**

Muhammad Saad Khilji, Sophie Emilie Bresson, Danielle Verstappen, Celina Pihl, Phillip Alexander Keller Andersen, et al.. The inducible  $\beta 5i$  proteasome subunit contributes to proinsulin degradation in GRP94 deficient  $\beta$  cells and is overexpressed in type 2 diabetes pancreatic islets. *American Journal of Physiology. Endocrinology Metabolism and Gastrointestinal Physiology*, 2020, 318 (6), pp.e892-e900. 10.1152/ajpendo.00372.2019 . hal-03019431

**HAL Id: hal-03019431**

**<https://cnrs.hal.science/hal-03019431>**

Submitted on 23 Mar 2021

**HAL** is a multi-disciplinary open access archive for the deposit and dissemination of scientific research documents, whether they are published or not. The documents may come from teaching and research institutions in France or abroad, or from public or private research centers.

L'archive ouverte pluridisciplinaire **HAL**, est destinée au dépôt et à la diffusion de documents scientifiques de niveau recherche, publiés ou non, émanant des établissements d'enseignement et de recherche français ou étrangers, des laboratoires publics ou privés.

1 **The inducible  $\beta$ 5i proteasome subunit contributes to proinsulin degradation in GRP94**  
2 **deficient  $\beta$ -cells and is overexpressed in type 2 diabetes pancreatic islets**

3 Muhammad Saad Khilji<sup>1</sup>, Sophie Emilie Bresson<sup>1</sup>, Danielle Verstappen<sup>1,2</sup>, Celina Pihl<sup>1</sup>, Phillip  
4 Alexander Keller Andersen<sup>1</sup>, Jette Bach Agergaard<sup>1</sup>, Tina Dahlby<sup>1</sup>, Tenna Holgersen Bryde<sup>1</sup>,  
5 Kristian Klindt<sup>1</sup>, Christian Kronborg Nielsen<sup>1</sup>, Anna Walentinsson<sup>3</sup>, Dusan Zivkovic<sup>4</sup>, Marie-Pierre  
6 Bousquet<sup>4</sup>, Björn Tyrberg<sup>5,6</sup>, Sarah J Richardson<sup>7</sup>, Noel G Morgan<sup>7</sup>, Thomas Mandrup-Poulsen<sup>1</sup>,  
7 Michal Tomasz Marzec<sup>1\*</sup>

8

9 Affiliations

10 <sup>1</sup> Laboratory of Immuno-endocrinology, Inflammation, Metabolism and Oxidation Section,  
11 Department of Biomedical Sciences, University of Copenhagen, Copenhagen, Denmark

12 <sup>2</sup> Radboud Universiteit, Nijmegen, Netherlands

13 <sup>3</sup> Translational Science & Experimental Medicine, Early Cardiovascular, Renal and Metabolism,  
14 BioPharmaceuticals R&D, AstraZeneca, Gothenburg, Sweden.

15 <sup>4</sup> Institut de Pharmacologie et de Biologie Structurale, Centre National de la Recherche Scientifique,  
16 Université de Toulouse, 31077 Toulouse, France

17 <sup>5</sup> Department of Physiology, Institute of Neuroscience and Physiology, Sahlgrenska Academy,  
18 University of Gothenburg, Gothenburg, Sweden

19 <sup>6</sup> Current affiliation: Cardiovascular and Metabolic Diseases, Institute de Recherches Servier,  
20 Suresnes, France

21 <sup>7</sup> Institute of Biomedical and Clinical Sciences, University of Exeter Medical School, Exeter, UK

22

23

24 *\*Corresponding author:*

25 Associate Professor Michal Tomasz Marzec M.D., PhD.

26 Postal Address: Panum Institut 12.6.10, Blegdamsvej 3B, DK-2200 Copenhagen, Denmark

27 Phone: +45 25520256

28 Email: [Michal@sund.ku.dk](mailto:Michal@sund.ku.dk)

29 **Keywords:**  $\beta$ 5i, proteasome, proinsulin degradation, GRP94, restoration of proinsulin

30

31 **Abstract**

32 Proinsulin is a misfolding-prone protein and its efficient breakdown is critical, when  $\beta$ -cells are  
33 confronted with high insulin biosynthetic demands, to prevent endoplasmic reticulum stress, a key  
34 trigger of secretory dysfunction and, if uncompensated, apoptosis. Proinsulin degradation is thought  
35 to be performed by the constitutively expressed standard proteasome, while the roles of other  
36 proteasomes are unknown. We recently demonstrated that deficiency of the proinsulin chaperone  
37 GRP94 causes impaired proinsulin-handling and defective insulin-secretion associated with a  
38 compensated endoplasmic reticulum stress-response. Taking advantage of this model of restricted  
39 folding-capacity, we investigated the role of different proteasomes in proinsulin degradation,  
40 reasoning that insulin secretory dynamics require an inducible protein degradation-system.

41 We show that expression of only one enzymatically active proteasome subunit, namely the  
42 inducible  $\beta 5i$ -subunit, was increased in GRP94 CRISPR/Cas9 KO cells. Additionally, the level of  
43  $\beta 5i$  containing intermediate proteasomes was significantly increased in these cells, as was  $\beta 5i$ -  
44 related chymotrypsin-like activity. Moreover, proinsulin levels were restored in GRP94 KO upon  
45  $\beta 5i$  siRNA-mediated knock down. Finally, the fraction of  $\beta$ -cells expressing  $\beta 5i$  subunit is increased  
46 in human islets from type 2 diabetes patients. We conclude that  $\beta 5i$  is an inducible proteasome  
47 subunit dedicated to the degradation of mishandled proinsulin.

48

49

50

51

52

53

54

## 55 **1. Introduction**

56 The insulin secretory dynamics and associated transients in proinsulin biosynthesis endanger the  
57 pancreatic  $\beta$ -cells for the detrimental consequences of protein misfolding. Even in normal  
58 conditions 20 % of proinsulin is misfolded, implicating that  $\beta$ -cells critically depend upon a highly  
59 flexible protein degradation system to avoid endoplasmic reticulum (ER) stress, cellular dysfunction  
60 and death (24). Misfolded proinsulin is disposed from the ER through the Endoplasmic-Reticulum-  
61 Associated protein Degradation (ERAD) pathway with final proteolysis performed by the  
62 proteasome (10). There are four major types of proteasomes that differ in composition of  $\beta$  subunits  
63 forming the enzymatically active inner rings of the 20S proteasome core: the constitutively  
64 expressed standard proteasome (composed of  $\beta$ 1,  $\beta$ 2,  $\beta$ 5; s-proteasome), the immunoproteasome  
65 ( $\beta$ 1i,  $\beta$ 2i,  $\beta$ 5i), the intermediate proteasome (containing a combination of standard and inducible  $\beta$   
66 subunits; int-proteasome) and the thymus-specific proteasome (containing  $\beta$ 5t subunit) (17).  
67 Inducible subunits are constitutively expressed not only in immune cells but also in the pancreatic  
68 islets, as reported recently by us and the Human Protein Atlas database (11, 26). Expression of the  
69 inducible subunits in  $\beta$ -cells is further upregulated by cytokines e.g.  $\text{INF}\gamma/\beta$  and  $\text{IL-1}\beta$  (6, 11, 15)  
70 during viral infections (16), and their constitutive expression has also been reported in e.g. heart and  
71 liver where they form int-proteasomes constituting 1-50% of total proteasomes of a cell (4, 8, 21).  
72 However, the role of non-standard proteasomes in proinsulin degradation has not been investigated.  
73 Most studies of proteasome biology employ broad-spectrum proteasome inhibitors such as MG132  
74 and lactacystin (9, 13) that cannot clarify the roles of individual proteasome subunits in protein  
75 degradation. Moreover,  $\beta$ -cell investigative models have focused on the fate of *mutated* e.g. AKITA  
76 proinsulin and not on misfolded *wild-type* proinsulin, as it has been assumed that the relevant  
77 degradation mechanisms are similar if not identical (9).

78 We recently showed that Glucose Regulated Protein 94 (GRP94), an ER resident chaperone, is  
79 critical for proinsulin handling. Deficient GRP94 activity results in substantial loss of intracellular  
80 proinsulin and a reduction in insulin secretion (7). As the loss of proinsulin in GRP94 knockout  
81 (KO) cells occurs at the level of ER (7), we hypothesized that mishandled proinsulin becomes an  
82 ERAD and proteasome substrate.

83 We therefore examined the activity and composition of proteasome(s) in GRP94 KO clonal cell  
84 lines derived from  $\beta$ -cell line Ins1-E and showed that these cells specifically overexpress the  
85 inducible  $\beta 5i$  proteasome subunit that is incorporated into enzymatically active proteasomes.  
86 Furthermore, siRNA-based reduction of  $\beta 5i$  expression increased intracellular levels of proinsulin.  
87 Finally, we demonstrated that the  $\beta 5i$  subunit is expressed in an increased fraction of  $\beta$ -cells from  
88 type 2 diabetes patients.

89

## 90 **2. Methods**

91 **Cell culture** Ins1-E GRP94 KO cells were generated as described in (7). The cells were grown in  
92 RPMI-1640 (Life Technologies, Naerum, Denmark) supplemented with 10 % fetal bovine serum  
93 (FBS), 1 % Penicillin/Streptomycin (P/S), 10 mM N-2-hydroxyethylpiperazine-N-2-ethane sulfonic  
94 acid (HEPES), 50  $\mu$ M  $\beta$ -mercaptoethanol and 1 mM sodium pyruvate, on fibronectin coated  
95 plasticware. The GRP94 inhibitor PU-WS13 (GRP94i) was described in (19) and used as in (7).

96 **Western Blotting** Cells were lysed and protein concentration calculated as in (7). Samples were run  
97 on Nu-Page 4-12 % bis-tris gels (Thermo Fisher Scientific, Hvidovre, Denmark), transferred to  
98 PVDF membranes before an overnight incubation with primary antibodies (Abcam:  $\beta 5i$  ab183506,  
99  $\beta 2i$  ab3329,  $\beta 1i$  ab243556; Sigma:  $\beta 1$  HPA029635,  $\beta 2$  HPA026322,  $\beta 5$  SAB210895,  
100 Thermo Fisher scientific: GRP94 MA3-016, Santa Cruz biotech: Tubulin T6074; Cell Signaling:

101 Insulin 8138S). Blots were developed using chemiluminescence and captured using the  
102 Azure<sup>®</sup>Saphire Biomolecular Imager. Quantification of Western blots was by ImageJ software  
103 (v.1.52a, (22)).

104 **Proteasome activity assay** GRP94 KO and control cells were plated in 96-well plates, treated with  
105 50 nM ONX-0914 (Selleck Chemicals, Rungsted, Denmark, IC50:~10 nM for  $\beta$ 5i, (18)) or vehicle-  
106 containing control medium for 2 h prior to experiments. As previously described (15)  
107 chymotrypsin-, trypsin- and caspase-like activities were measured through luminescent assay using  
108 Proteasome-GloTM Assay (Promega, Nacka, Sweden). Statistical analysis was done on the average  
109 of each biological triplicate each point represented by a technical replicate.

110 **Proteasome Mass-spectrometry analysis** Cells were grown to 90 % confluence, washed with  
111 Hank's Balanced Salt Solution (HBSS) before incubation with culture media supplemented with 0.1  
112 % formaldehyde for cross-linking for 15 minutes. Next, 125 mM glycine was added for 10 minutes  
113 at 37°C to quench the formaldehyde. The cells were then washed with HBSS, centrifuged and  
114 pellets stored at -80°C. Immuno-purification of the proteasomes from the *in vivo* cross-linked  
115 lysates, liquid chromatography mass spectrometry (LC-MS/MS) analysis, protein identification,  
116 validation and quantifications were performed as previously described (2, 4). Briefly, proteasomes  
117 were purified by incubating the lysates with CNBr sepharose beads (GE Healthcare) covalently  
118 bound to the antibody specific for the  $\alpha$ 2 subunit of the proteasome (MCP21), using 150 million  
119 cells per 50 mg of grafted beads. Two additional cycles of purification were conducted, re-  
120 incubating the collected supernatant with antibody-grafted beads. All fractions were pooled and LC-  
121 MS/MS analysis performed.

122 **Single-Cell RNA Sequencing of Pancreatic Islets** Pancreatic islet cell subpopulations were  
123 analyzed for  $\beta$ 5i,  $\beta$ 1i and  $\beta$ 2i expression with human islet single-cell sequencing data (23). FastQ

124 files were downloaded from ArrayExpress (accession: E-MTAB-5061). Data was analyzed with  
125 bcbio nextgen (<https://github.com/chapmanb/bcbio-nextgen>), using the hisat2 algorithm (12) to  
126 align reads to human genome version hg38 and the Salmon algorithm (20) for quantitation of gene  
127 counts.

128 **β5i siRNA-mediated knockdown** GRP94 KO cells were grown in 6-well plates to 80 %  
129 confluence and transfected with β5i-directed SMART-POOL siRNA (Dharmacon®, Cambridge,  
130 Great Britain), using the Lipofectamine 3000 transfection kit according to manufacturer's protocol  
131 (Thermo Fisher Scientific, Hvidovre, Denmark). Supernatants were collected for measurements of  
132 proinsulin and insulin by ELISAs (Cat. #10-1232-01 and 10-1250-01, Merckodia, Uppsala, Sweden)  
133 according to manufacturer's protocols. Cell viability assay was performed using the staining reagent  
134 AlamarBlue (Life Technologies, Naerum, Denmark) added to the cell culture for 4h, incubated at  
135 37°C. The resulting fluorescence was read at 570 nm and 600 nm (reference) on a plate reader.  
136 Thapsigargin was used at the dose of 0.1 μM for 24 h.

137 **Real-time Quantitative PCR** RNA was isolated using the NucleoSpin® RNA kit (Macherey-  
138 Nagel, Bethlehem, USA), followed by cDNA synthesis (iScript™ cDNA Synthesis Kit BioRad,  
139 Copenhagen, Denmark) and quantification using SYBR® Green master mix (Life Technologies  
140 Naerum, Denmark). The primers used: PSMB8 (F: CCAGGAAAGGAAGGTTTCAGAT, R:  
141 ATCTCGATCACCTTGTTTCAC); ins-1 (F: GGGGAACGTGGTTTCTTCTAC, R:  
142 CCAGTTGGTAGAGGGAGCAG); ins-2 (F: CAGCACCTTTGTGGTTCTCA, R:  
143 CACCTCCAGTGCCAAGGT); HPRT1 (F: GCAGACTTTGCTTTCCTT, R:  
144 CCGCTGTCTTTTAGGCTT); β-actin (F: CACCCGCGAGTACAACCTTC, R:  
145 CCCATACCCACCATCACACC); PPIA (F: AGCACTGGGGAGAAAGGATT, R:  
146 GATGCCAGGACCTGTATGCT). The best reference genes for normalization were determined as



147 in (1), and normalization was carried out using the  $2^{(-\Delta CT)}$  method to provide the relative gene  
148 expression levels.

149 **Donor human islets** were received at 90 % purity from the European Consortium for Islet  
150 Transplantation (ECIT). Donor information: female, 56 y.o., BMI 19.4, cause of death was cerebral  
151 bleeding, blood group A+, HLA (A:B) 1,29 : 18,57, HLA (DR) 11,11, cold ischemia time 4 h, time  
152 for islets isolation to shipment 16 h, estimated purity 80 %. After a 24 h pre-incubation in RPMI  
153 medium supplemented with 10 % FBS, 1 % P/S and 5.6 mM glucose, 500 islets per experimental  
154 condition were transferred to RPMI medium supplemented with 1 % HS and 24 h later experiments  
155 were performed.

156 **Statistical analysis** Quantified data of Western blots and proteasome assays were assessed by  
157 Bonferroni corrected two-tailed Student's t-test. GraphPad Prism (v. 7.04, La Jolla, CA, USA) was  
158 used for all statistical analyses and data presentation. Data is presented as means  $\pm$  SD with p-  
159 values of  $\leq 0.05$  considered significant.

### 160 **3. Results**

#### 161 **Increased expression and activity of $\beta 5i$ in GRP94 KO cells**

162 To investigate the expression of enzymatically active proteasome  $\beta$  subunits, we analyzed protein  
163 contents of GRP94 KO and control clonal cell lines. We found all standard and inducible  $\beta$  subunits  
164 expressed to varying degrees in the tested cells (Fig. 1) but only the  $\beta 5i$  subunit was expressed  
165 significantly more in GRP94 KO cells compared to controls (Fig. 1A-B).  $\beta 5i$  mRNA was  
166 upregulated in a similar fashion in GRP94 KO cells (Fig. 1C).

167 Next, we measured levels of overall substrate-specific proteasome activities. GRP94 KO cells  
168 showed increased chymotrypsin-like activity (characteristic for  $\beta 5$ ,  $\beta 5i$ ,  $\beta 1i$  subunits (25)) compared  
169 to the control group while the other substrate-specific activities remained unchanged (Fig. 1F).

170 Treatment of cells for 2 h with 50 nM of ONX-0914, a  $\beta 5i$  specific inhibitor, reduced  
171 chymotrypsin-like activity in the GRP94 KO to the levels observed in control cells treated with  
172 ONX-0914, indicating that increase in this type of activity is  $\beta 5i$  dependent (Fig. 1F).

### 173 **Increased incorporation of $\beta 5i$ subunit into active proteasomes in GRP94 KO cells**

174 Next, we investigated the cellular composition of proteasomes through immunoprecipitation (IP) of  
175 the 20S  $\alpha 2$  proteasome subunit followed by LC-MS/MS analysis. We identified the presence of two  
176 types of proteasomes: the s-proteasome and int-proteasome, containing  $\beta 1$ ,  $\beta 2$ ,  $\beta 5$  and  $\beta 1$ ,  $\beta 2$ ,  $\beta 5i$   
177 subunits respectively, with no other detectable inducible subunits incorporated (Fig. 2A). The s-  
178 proteasome was the dominant form present in control (83.2 %) and GRP94 KO cells (79.9 %). Int-  
179 proteasome represented 16.8% of proteasomes in control group while its presence was increased to  
180 20.1% in GRP94 KO cells. Furthermore, we identified a significant increase in the 11S regulatory  
181 particles (PA28 $\alpha\beta$  and PA200), known to be part of the immunoproteasomes (3), in active  
182 proteasomes of GRP94 KO cells (Fig. 2B).

### 183 **Inhibition of $\beta 5i$ activity increases proinsulin levels in GRP94 KO cells**

184 As  $\beta 5i$  was the only proteasome subunit upregulated in GRP94 KO cells and incorporated into  
185 active proteasomes to a higher degree, we evaluated the possible role of the  $\beta 5i$  subunit in  
186 proinsulin degradation in GRP94-deficient cells.  $\beta 5i$  was knocked down with three individual  
187 siRNAs (Fig. 2C). Concurrently, levels of intracellular proinsulin and mature insulin increased as  
188 compared to siRNA control treated cells (Fig. 2D) with no apparent upregulation in *Ins1-2* genes  
189 transcription (Fig. 2E). The observed increase was accompanied by higher amount of constitutively  
190 secreted proinsulin but not insulin (experiment was performed in 2 mM glucose containing media;  
191 Fig. 2F). Finally,  $\beta 5i$  KD induced partial loss of cell viability (Fig. 2G).

### 192 **$\beta 5i$ expression is increased upon glucose stimulation and GRP94 ATP-ase inhibition**

193 In order to mimic increased insulin demand conditions and increased proinsulin production, Ins1-E  
194 cells and human islets were cultured in the presence of 20 mM glucose. As expected, intracellular  
195 proinsulin levels increased accompanied by the smaller increase in insulin levels, presumably  
196 because mature insulin is secreted at 20 mM glucose concentration. After 24 and 48 h we observed  
197 10-25 % increase in the  $\beta 5i$  expression (Fig. 3A, n=3 and 3B, n=1), induced further by the addition  
198 of 5-20  $\mu$ M of GRP94i (Fig. 3C; n=1). Off note, proinsulin and insulin levels were diminished after  
199 treatment with GRP94i, as reported previously (7). At this point, human islets results should be  
200 taken with a reservation as they represent only a single experiment with a single islet donor.

#### 201 **$\beta 5i$ expression is increased in pancreatic islet cells in type 2 diabetes**

202 To investigate whether inducible  $\beta$  subunits are overexpressed in islets of type 2 diabetes (T2D)  
203 patients, we analyzed RNA-sequencing data of single-cells dispersed from pancreatic islets (23).  
204 We found that 20 % more of  $\alpha$ -, and 40 % more of  $\beta$ - and  $\delta$ -cells from T2D patients tested positive  
205 for expression of the  $\beta 5i$  subunit compared to non-diabetic controls (Fig. 4A). Similarly, 10 % more  
206 of all islet cell-types were  $\beta 1i$ -positive in T2D compared to control cases (Fig. 4B) with no  
207 significant changes observed for  $\beta 2i$  (Fig. 4C). When  $\beta 5i$ - (and  $\beta 2i$ -) positive cells were analyzed  
208 for expression levels of  $\beta$  subunits, we found no significant changes (Fig 4D) between control and  
209 T2D cases. The  $\beta 1i$  subunit exhibited lower expression in T2D cases but significance was reached  
210 only in  $\alpha$ -cells (Fig. 4E).

211 Next, we analyzed the inter-dependence between GRP94 and  $\beta 5i$  expression and found statistically  
212 significant correlation only in  $\beta$ -cells but the correlation was weak ( $R^2=0.2$ ) indicating that only a  
213 fraction of  $\beta$ -cells exhibited the inter-dependence in expression of these genes (Fig. 4G-I).

214

#### 215 **4. Discussion**

216 Here, we report that the expression of the inducible proteasome subunit  $\beta 5i$  was significantly higher  
217 in GRP94 KO cells, a  $\beta$ -cell model of restricted ER folding capacity and proinsulin mishandling,  
218 and in islets of T2D patients. Moreover, we have shown that proteasomes containing the  $\beta 5i$  subunit  
219 are engaged in proinsulin degradation.

220 Misfolded proinsulin has been thought to be degraded by the s-proteasome but the experimental  
221 procedures employed have not been able to distinguish proteasome subtypes involved in the process  
222 (9, 10, 13). Low levels of intracellular proinsulin, accompanied by unaffected preproinsulin  
223 transcription in GRP94 KO (7) indicate enhanced proinsulin degradation. We expected a broad  
224 upregulation of expression of proteasome subunits to counteract a higher load of mishandled  
225 proinsulin. Unexpectedly, we show that limiting folding capacity (GRP94 KO) induces  
226 upregulation of only  $\beta 5i$  expression (Fig. 1A). The increase in  $\beta 5i$  expression was accompanied by  
227 an increase in chymotrypsin-like activity in GRP94 KO that was reduced as a result of the treatment  
228 with a  $\beta 5i$  selective small-molecule inhibitor, ONX-0194 (Fig. 1F). The particular position of the  
229  $\beta 5i$  in the inducible proteasomal response in  $\beta$ -cells was confirmed by mass spectrometry showing  
230 increased presence of  $\beta 5i$ -containing int-proteasomes in GRP94 KO cells (Fig. 2A). We did not  
231 detect incorporation of other inducible  $\beta$  subunits despite their demonstrated expression in control  
232 and GRP94 KO cells (Fig. 1). Finally, we showed that  $\beta 5i$  can be upregulated in response to  
233 prolonged exposure to high glucose concentration and ATP-ase inhibition of GRP94 activity that  
234 mimics the limited  $\beta$ -cell folding capacity (Fig. 3, note that human islets experiments represent  $n=1$   
235 and thus should be viewed with caution).

236 The increased presence of the  $\beta 5i$  subunit containing int-proteasomes likely signifies the evolution  
237 of a positive and inducible adaptive response dedicated to proinsulin degradation under conditions  
238 of biosynthetic stress. Conversely, we showed that  $\beta 5i$  KD results in an increase in intracellular  
239 proinsulin and insulin (Fig. 2C and D) and loss of cell viability (Fig. 2G).

240 What signaling processes could be responsible for the changes in subunits expression? Our  
241 experiments were performed with Ins-1E cells *in vitro* and therefore the upregulation of the  
242 expression of  $\beta 5i$  had to occur in non-stimulated conditions with cells employing internal  
243 mechanisms to upregulate it. Theoretically, constitutive activation of NACHT, LRR and PYD  
244 domains-containing protein 3 (NLRP3)-inflammasome may be involved. Classically, this activation  
245 requires signal-1 that increases intracellular pro-interleukin (IL)-1 $\beta$  concentration in response to  
246 binding of ligands to toll-like receptors (TLR) and signal-2 that triggers inflammasome-dependent  
247 activation of caspase-1 that in turn processes pro-IL-1 $\beta$  into the mature biologically active cytokine.  
248 Some substances can provide both signal-1 and 2 (27) and these include ER stress-inducing drugs  
249 such as thapsigargin (14). We have previously reported that GRP94 KO cells mount a compensated  
250 ER stress, with a limited PERK response (7) that would lead to increased inflammasome activity  
251 through TXNIP (as in (5)), and production of IL-1 $\beta$ . We have recently showed that externally  
252 provided non-toxic concentrations of IL-1 $\beta$  induce expression of  $\beta 5i$  and  $\beta 1i$  in Ins-1E cells and  
253 mouse and human islets (11). How that result relates to those reported here, with overexpression of  
254 only  $\beta 5i$ , remains to be clarified.

255 T2D patients exhibited increased fractions of  $\alpha$ -,  $\beta$ - and  $\delta$ -cells expressing  $\beta 5i$  mRNA (Fig.4A) and  
256 weak but significant correlation between increased GRP94 and  $\beta 5i$  mRNAs in T2D. As the demand  
257 for insulin biosynthesis increases during the progression of T2D,  $\beta$ -cells respond by increasing  
258 proinsulin synthesis and upregulating folding machinery. Despite that compensation, T2D patients  
259 display increased proinsulin misfolding. The observed  $\beta 5i$  upregulation is therefore likely a positive  
260 adaptive mechanism that through the increased degradation of mishandled proinsulin contributes to  
261  $\beta$ -cell homeostasis.

262 The role of specific proteasomes in proinsulin degradation remains to be uncovered in detail and  
263 our results do not preclude involvement of s-proteasomes in this process. However, the perspective

264 that in a compromised ER folding environment in islets of T2D patients,  $\beta$ -cells specifically  
265 overexpress and incorporate the  $\beta 5i$  proteasome subunit into inducible int-proteasomes that  
266 contributes to proinsulin degradation warrants further investigation into its significance for human  
267 cases.

268

## 269 **5. Funding**

270 This study was funded by The Punjab Educational Endowment Fund (M.S.K), the Danish Diabetes  
271 Academy supported by the Novo Nordisk Foundation (T.D), the Department of Biomedical  
272 Sciences at the University of Copenhagen (T.D., and M.T.M.); the Augustinus Foundation (T.D.  
273 and M.T.M.); European Foundation for the Study of Diabetes/Lilly European Diabetes Research  
274 Programme, Vissing Fonden, Bjarne Jensen Fonden, Kirsten og Freddy Johansens Fond (M.T.M.).

275

## 276 **6. Disclosures**

277 The authors declare that there are no conflicts of interests except for AW who is an employee of  
278 AstraZeneca and has shares in the company.

279

## 280 **7. Author Contributions**

281 MSK, SEB, DV, THB, CP, PAKA, JBA, CKN, KK developed the protocols, conducted  
282 experiments, the statistical analysis, constructed figure, wrote and reviewed the manuscript. TD  
283 developed GRP94 KO clones and participated in writing the manuscript. Bioinformatics analysis of  
284 single-cell RNA-sequencing data was conducted by AW and BT. M-PB and DZ performed and  
285 analyzed mass spectrometry and wrote the manuscript. SJR and NGM performed human islet

286 related experiments and participated in critical analysis of the data. TMP developed the protocols,  
287 participated in data analysis and writing the manuscript. MTM is the study guarantor and was its  
288 initiator; developed the protocols, performed the statistical analysis and constructed figures and  
289 tables as well as wrote the manuscript.

## 290 REFERENCES

- 291 1. **Andersen CL, Jensen JL, and Orntoft TF.** Normalization of real-time quantitative  
292 reverse transcription-PCR data: a model-based variance estimation approach to identify genes  
293 suited for normalization, applied to bladder and colon cancer data sets. *Cancer research* 64: 5245-  
294 5250, 2004.
- 295 2. **Bertrand Fabre TL, David Bouyssié, Thomas Menneteau, Bernard Monsarrat,**  
296 **Odile Burlet-Schiltz, Marie-Pierre Bousquet-Dubouch.** Comparison of label-free quantification  
297 methods for the determination of protein complexes subunits stoichiometry. *EuPA Open Proteomics*  
298 4: 82-86, 2014.
- 299 3. **Fabre B, Lambour T, Garrigues L, Amalric F, Vigneron N, Menneteau T, Stella**  
300 **A, Monsarrat B, Van den Eynde B, Burlet-Schiltz O, and Bousquet-Dubouch MP.** Deciphering  
301 preferential interactions within supramolecular protein complexes: the proteasome case. *Mol Syst*  
302 *Biol* 11: 771, 2015.
- 303 4. **Fabre B, Lambour T, Garrigues L, Ducoux-Petit M, Amalric F, Monsarrat B,**  
304 **Burlet-Schiltz O, and Bousquet-Dubouch MP.** Label-free quantitative proteomics reveals the  
305 dynamics of proteasome complexes composition and stoichiometry in a wide range of human cell  
306 lines. *Journal of proteome research* 13: 3027-3037, 2014.
- 307 5. **Fan P, Tyagi AK, Agboke FA, Mathur R, Pokharel N, and Jordan VC.**  
308 Modulation of nuclear factor-kappa B activation by the endoplasmic reticulum stress sensor PERK  
309 to mediate estrogen-induced apoptosis in breast cancer cells. *Cell Death Discov* 4: 15, 2018.
- 310 6. **Freudenburg W, Gautam M, Chakraborty P, James J, Richards J, Salvatori AS,**  
311 **Baldwin A, Schriewer J, Buller RM, Corbett JA, and Skowyra D.** Reduction in ATP levels  
312 triggers immunoproteasome activation by the 11S (PA28) regulator during early antiviral response  
313 mediated by IFNbeta in mouse pancreatic beta-cells. *PloS one* 8: e52408, 2013.
- 314 7. **Ghiasi SM, Dahlby T, Hede Andersen C, Haataja L, Petersen S, Omar-Hmeadi**  
315 **M, Yang M, Pihl C, Bresson SE, Khilji MS, Klindt K, Cheta O, Perone MJ, Tyrberg B, Prats**  
316 **C, Barg S, Tengholm A, Arvan P, Mandrup-Poulsen T, and Marzec MT.** Endoplasmic  
317 Reticulum Chaperone Glucose-Regulated Protein 94 Is Essential for Proinsulin Handling. *Diabetes*  
318 68: 747-760, 2019.
- 319 8. **Guillaume B, Chapiro J, Stroobant V, Colau D, Van Holle B, Parvizi G,**  
320 **Bousquet-Dubouch MP, Theate I, Parmentier N, and Van den Eynde BJ.** Two abundant  
321 proteasome subtypes that uniquely process some antigens presented by HLA class I molecules.  
322 *Proc Natl Acad Sci U S A* 107: 18599-18604, 2010.
- 323 9. **Hoelen H, Zaldumbide A, van Leeuwen WF, Torfs EC, Engelse MA, Hassan C,**  
324 **Lebbink RJ, de Koning EJ, Ressing ME, de Ru AH, van Veelen PA, Hoeben RC, Roep BO,**  
325 **and Wiertz EJ.** Proteasomal Degradation of Proinsulin Requires Derlin-2, HRD1 and p97. *PLoS*  
326 *One* 10: e0128206, 2015.
- 327 10. **Hu Y, Gao Y, Zhang M, Deng KY, Singh R, Tian Q, Gong Y, Pan Z, Liu Q,**  
328 **Boisclair YR, and Long Q.** Endoplasmic Reticulum-Associated Degradation (ERAD) Has a  
329 Critical Role in Supporting Glucose-Stimulated Insulin Secretion in Pancreatic beta-Cells. *Diabetes*  
330 68: 733-746, 2019.
- 331 11. **Khilji MS, Verstappen D, Dahlby T, Burstein Prause MC, Pihl C, Bresson SE,**  
332 **Bryde TH, Keller Andersen PA, Klindt K, Zivkovic D, Bousquet-Dubouch MP, Tyrberg B,**  
333 **Mandrup-Poulsen T, and Marzec MT.** The intermediate proteasome is constitutively expressed in  
334 pancreatic beta cells and upregulated by stimulatory, low concentrations of interleukin 1 beta. *PloS*  
335 *one* 15: e0222432, 2020.



- 336 12. **Kim D, Langmead B, and Salzberg SL.** HISAT: a fast spliced aligner with low  
337 memory requirements. *Nature methods* 12: 357-360, 2015.
- 338 13. **Kitiphongspattana K, Mathews CE, Leiter EH, and Gaskins HR.** Proteasome  
339 inhibition alters glucose-stimulated (pro)insulin secretion and turnover in pancreatic {beta}-cells. *J*  
340 *Biol Chem* 280: 15727-15734, 2005.
- 341 14. **Lerner AG, Upton JP, Praveen PV, Ghosh R, Nakagawa Y, Igbaria A, Shen S,**  
342 **Nguyen V, Backes BJ, Heiman M, Heintz N, Greengard P, Hui S, Tang Q, Trusina A, Oakes**  
343 **SA, and Papa FR.** IRE1alpha induces thioredoxin-interacting protein to activate the NLRP3  
344 inflammasome and promote programmed cell death under irremediable ER stress. *Cell Metab* 16:  
345 250-264, 2012.
- 346 15. **Lundh M, Bugliani M, Dahlby T, Chou DH, Wagner B, Ghiasi SM, De Tata V,**  
347 **Chen Z, Lund MN, Davies MJ, Marchetti P, and Mandrup-Poulsen T.** The immunoproteasome  
348 is induced by cytokines and regulates apoptosis in human islets. *The Journal of endocrinology* 233:  
349 369-379, 2017.
- 350 16. **McCarthy MK, and Weinberg JB.** The immunoproteasome and viral infection: a  
351 complex regulator of inflammation. *Front Microbiol* 6: 21, 2015.
- 352 17. **Morozov AV, and Karpov VL.** Biological consequences of structural and functional  
353 proteasome diversity. *Heliyon* 4: e00894, 2018.
- 354 18. **Muchamuel T, Basler M, Aujay MA, Suzuki E, Kalim KW, Lauer C, Sylvain C,**  
355 **Ring ER, Shields J, Jiang J, Shwonek P, Parlati F, Demo SD, Bennett MK, Kirk CJ, and**  
356 **Groettrup M.** A selective inhibitor of the immunoproteasome subunit LMP7 blocks cytokine  
357 production and attenuates progression of experimental arthritis. *Nat Med* 15: 781-787, 2009.
- 358 19. **Patel PD, Yan P, Seidler PM, Patel HJ, Sun W, Yang C, Que NS, Taldone T,**  
359 **Finotti P, Stephani RA, Gewirth DT, and Chiosis G.** Paralog-selective Hsp90 inhibitors define  
360 tumor-specific regulation of HER2. *Nature chemical biology* 9: 677-684, 2013.
- 361 20. **Patro R, Duggal G, Love MI, Irizarry RA, and Kingsford C.** Salmon provides fast  
362 and bias-aware quantification of transcript expression. *Nature methods* 14: 417-419, 2017.
- 363 21. **Pelletier S, Schuurman KG, Berkers CR, Ovaa H, Heck AJ, and Raijmakers R.**  
364 Quantifying cross-tissue diversity in proteasome complexes by mass spectrometry. *Mol Biosyst* 6:  
365 1450-1453, 2010.
- 366 22. **Rueden CT, Schindelin J, Hiner MC, DeZonia BE, Walter AE, Arena ET, and**  
367 **Eliceiri KW.** ImageJ2: ImageJ for the next generation of scientific image data. *BMC*  
368 *Bioinformatics* 18: 529, 2017.
- 369 23. **Segerstolpe A, Palasantza A, Eliasson P, Andersson EM, Andreasson AC, Sun X,**  
370 **Picelli S, Sabirsh A, Clausen M, Bjursell MK, Smith DM, Kasper M, Ammala C, and**  
371 **Sandberg R.** Single-Cell Transcriptome Profiling of Human Pancreatic Islets in Health and Type 2  
372 Diabetes. *Cell Metab* 24: 593-607, 2016.
- 373 24. **Sun J, Cui J, He Q, Chen Z, Arvan P, and Liu M.** Proinsulin misfolding and  
374 endoplasmic reticulum stress during the development and progression of diabetes. *Molecular*  
375 *aspects of medicine* 42: 105-118, 2015.
- 376 25. **Tanaka K.** The proteasome: overview of structure and functions. *Proc Jpn Acad Ser*  
377 *B Phys Biol Sci* 85: 12-36, 2009.
- 378 26. **Uhlen M, Fagerberg L, Hallstrom BM, Lindskog C, Oksvold P, Mardinoglu A,**  
379 **Sivertsson A, Kampf C, Sjostedt E, Asplund A, Olsson I, Edlund K, Lundberg E, Navani S,**  
380 **Szigyarto CA, Odeberg J, Djureinovic D, Takanen JO, Hober S, Alm T, Edqvist PH, Berling**  
381 **H, Tegel H, Mulder J, Rockberg J, Nilsson P, Schwenk JM, Hamsten M, von Feilitzen K,**  
382 **Forsberg M, Persson L, Johansson F, Zwahlen M, von Heijne G, Nielsen J, and Ponten F.**  
383 Proteomics. Tissue-based map of the human proteome. *Science* 347: 1260419, 2015.

384 27. **Wali JA, Gurzov EN, Fynch S, Elkerbout L, Kay TW, Masters SL, and Thomas**  
385 **HE.** Activation of the NLRP3 inflammasome complex is not required for stress-induced death of  
386 pancreatic islets. *PLoS One* 9: e113128, 2014.

387

388 **Figure 1. Expression and activity of proteasome  $\beta$  subunits.**

389 SDS-PAGE and Western blot analysis with quantification of relative levels of expression of  $\beta$   
390 inducible (**A-B**) and (**D-E**) standard proteasome subunits in Ins-1E derived GRP94 KO and control  
391 clonal cells (n=3). **C.** mRNA levels of  $\beta 5i$  gene were analyzed by quantitative reverse transcription-  
392 PCR (qRT-PCR) in control and GRP94 KO cells (n=6, individual clones data shown). **F.**  
393 Proteolytic-specific activities exhibited by proteasome subunits treated with  $\beta 5i$  subunit specific  
394 inhibitor ONX-0914 (2 h, 50 nM). Proteasome activity was evaluated in cultured cells and the data  
395 is shown as luminescence per cell. Statistical analysis performed by Bonferroni corrected unpaired  
396 two-tailed Student's t-test. The data are presented as means $\pm$ SD.

397

398 **Figure 2. Proteasome activity and structure in GRP94 KO clonal cells and an effect of  $\beta 5i$  KD**  
399 **on proinsulin/insulin contents.**

400 **A-B** Proteasomes were precipitated with anti-MCP21 from  $4 \times 10^8$  cells and analyzed by LC-  
401 MS/MS. The absolute quantities of each of the  $\beta$  subunits and regulatory particles measured by the  
402 LC-MS/MS method were computed to calculate the stoichiometry of 20S proteasome subtypes and  
403 20S proteasome-associated regulators, n=4. Statistical analysis performed by Bonferroni corrected  
404 unpaired two-tailed Student's t-test. **C-G** siRNA KD of  $\beta 5i$  in GRP94 KO cells was analyzed 72 h  
405 post siRNA delivery via: **C.** SDS-PAGE and Western blot analysis of proinsulin and insulin  
406 expression; **D.** quantification of WB data from six independent experiments; data depicted as  
407 percentage of control; **E.** mRNA levels of  $\beta 5i$  and *Ins-1-2* genes were analyzed by qRT-PCR in  
408 control and GRP94 KO cells (n=4); **F.** evaluation by ELISA assays of proinsulin and insulin  
409 secretion after additional 2 h culture in 2 mM glucose containing medium (n=3); **G.** Cell viability  
410 evaluated with AlamarBlue reagent. Thapsigargin was used at the dose of 0.1  $\mu$ M for 24 h (n=4).  
411 Statistical analysis performed by Bonferroni corrected paired two-tailed Student's t-test. The data is  
412 presented as means $\pm$ SD.

413

414 **Figure 3.  $\beta 5i$  expression is increased upon glucose stimulation and GRP94 ATP-ase inhibition.**

415 **A-C** Ins1-E cells and human islets from deceased donor were cultured in depicted glucose  
416 conditions for 24-48 h and their protein content analyzed by SDS-PAGE and Western blotting (3A:  
417 n=3 and 3B: n=1). **C.** Human islets were cultured for 24 h in the presence of 20 mM glucose and 20  
418  $\mu$ M of GRP94i and their content analyzed (n=1).

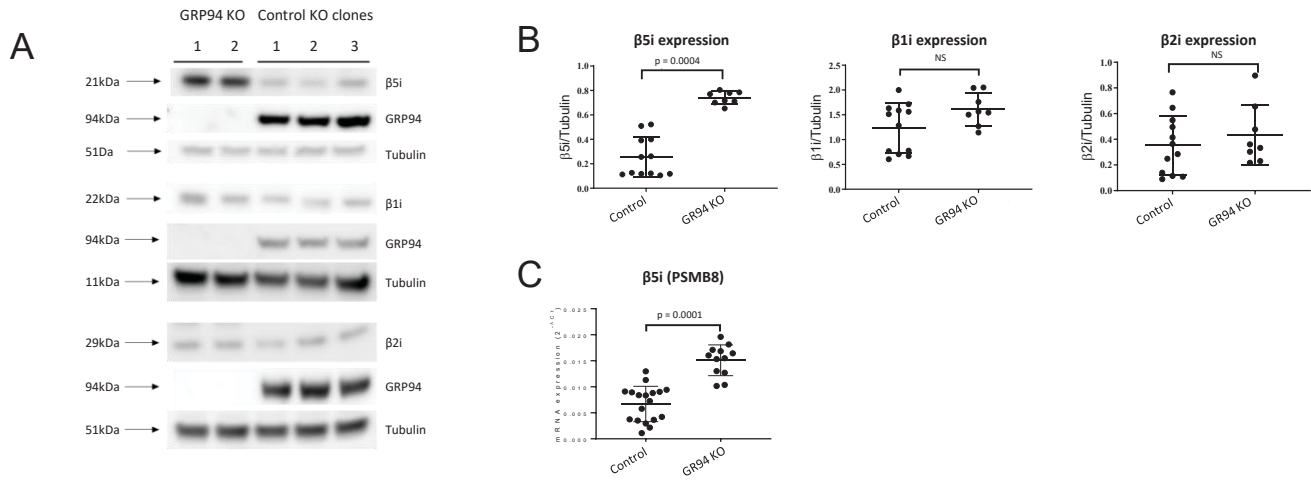
419

420 **Figure 4. Proteasome inducible subunits expression in islets of control and T2D patients. A-C**

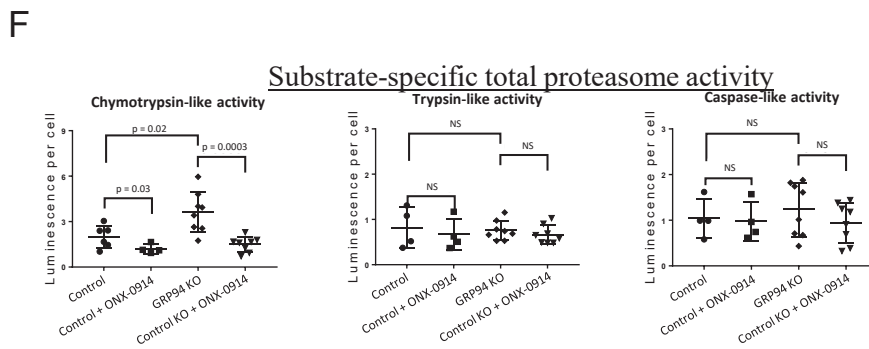
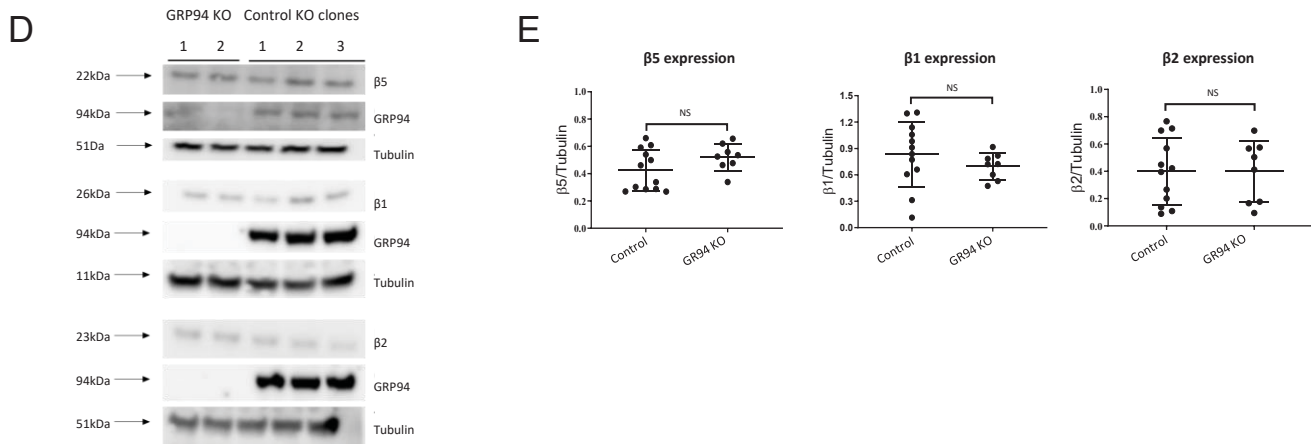
421 Single cell RNA sequencing analysis of  $\beta 5i$  (A),  $\beta 1i$  (B) and  $\beta 2i$  (C) gene expression in human  
422 pancreatic islets  $\alpha$ -,  $\beta$ - and  $\delta$ -cells from healthy individuals (n=6) and T2D patients (n=4). **D-F**  
423 Expression levels of inducible subunits were quantified as expression values (CPM, log2) per  
424 individual cell. Data is presented as means $\pm$ SD. **G-I** Pair-wise expression correlation between  
425 *GRP94 (HSP90B1)* and inducible subunit  $\beta 5i$  (*PSMB8*) expression in  $\alpha$ -,  $\beta$ - and  $\delta$ -cells from healthy  
426 and T2D patients (Pearson's correlation coefficients are shown; blue: healthy, green: T2D).  
427 Statistical analysis was performed using ANOVA with Bonferroni correction for multiple  
428 comparisons of T2D versus healthy donors.

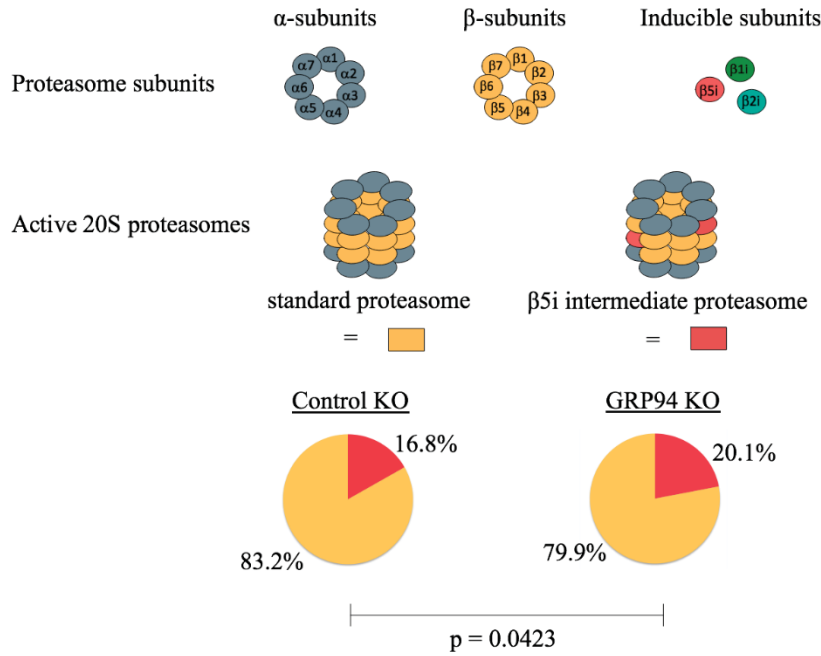
**Fig. 1**

Expression of inducible proteasome  $\beta$  subunits

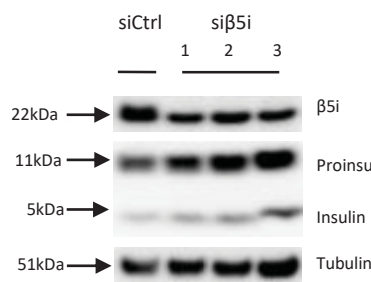
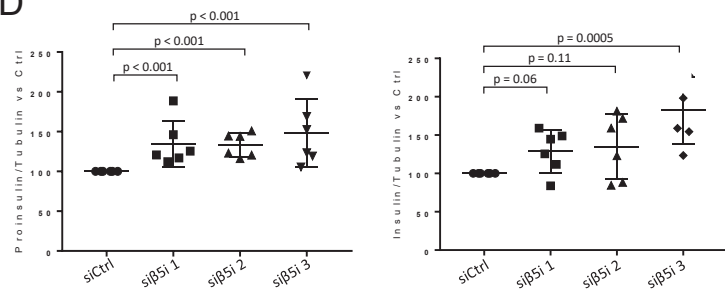
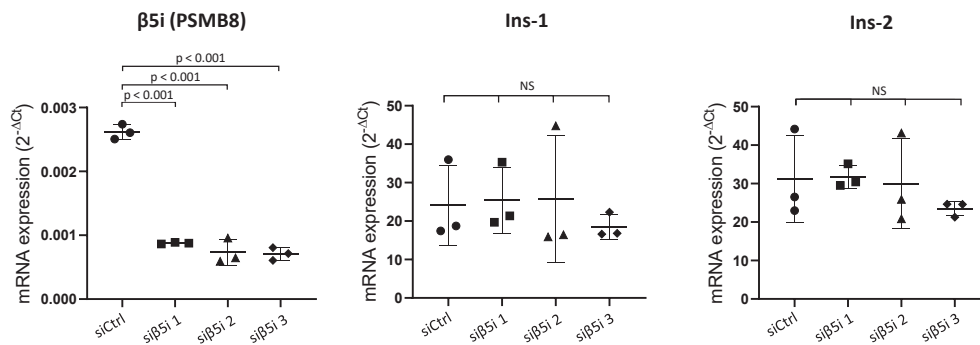
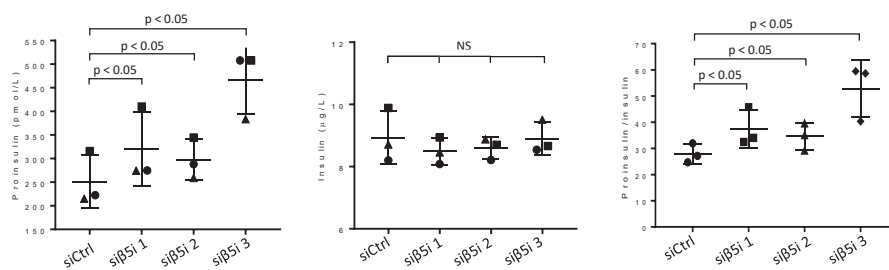
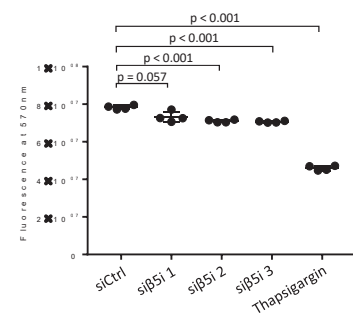


Expression of standard proteasome  $\beta$  subunits



**Fig. 2****Proteasome types detection by mass spectrometry****A****B**

Regulatory particle	GRP94 KO control	GRP94 KO	<i>p</i> value
19S	86.13	70.15	0.174
PA28 $\alpha\beta$ (11S)	1.93	3.4	0.045
PA28 $\gamma$ (11S)	1.53	1.5	0.614
PA200 (11S)	0.76	1.25	0.019

**siRNA-based knockdown of  $\beta 5i$  subunit- protein expression****C****D****siRNA-based knockdown of  $\beta 5i$  subunit – mRNA expression****E****F****siRNA-based knockdown of  $\beta 5i$  subunit – secretion****G****siRNA-based knockdown of  $\beta 5i$  subunit – cell viability**

**Fig. 3**

$\beta$ 5i expression upon glucose stimulation and/or GRP94 ATP-ase inhibition

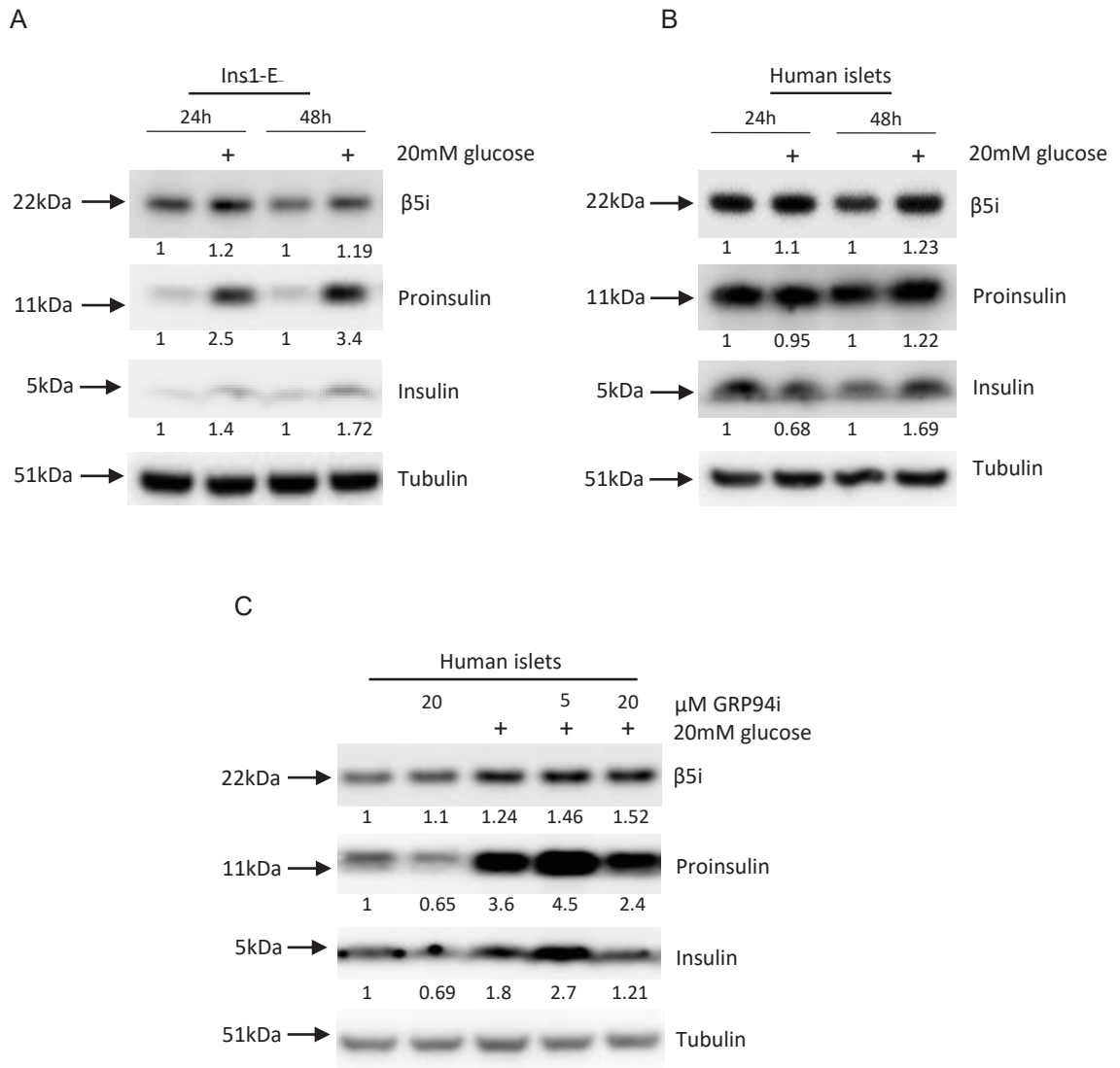


**Fig. 4**

mRNA sequencing of single cells from human islets

